Kapal: Jurnal Ilmu Pengetahuan dan Teknologi Kelautan
(Kapal: Journal of Marine Science and Technology)
journal homepage : http://ejournal.undip.ac.id/index.php/kapal
2301-9069 (e)
1829-8370 (p)

A Comprehensive Study of Renewable-Powered Floating Oil Skimmer Design for Indonesian Oil Spill Recovery

Ahmad Yasim[1*], Muhammad Irsan[2], Marfiansyah Nasra Dwiprayuda[2], Muh. Ikhsan[2], Muh. Fadil Zulkifli[1]

[1] Department of Naval Architecture, Bacharuddin Jusuf Habibie Institute of Technology, Parepare 91122, Indonesia
[2] Department of Energy Systems Engineering, Bacharuddin Jusuf Habibie Institute of Technology, Parepare 91122, Indonesia
[*] Corresponding Author: ahmadyasim@ith.ac.id

Article Info

Keywords:
Floating Platform;
Oil Skimmer;
Oil Spill Recovery;
Renewable Energy

Article history:
Received: 08/11/2025
Last revised: 21/04/2026
Accepted: 23/04/2026
Available online: 23/04/2026
Published: 28/04/2026

DOI:
https://doi.org/10.14710/kapal.v23i1.79027

Abstract

Indonesian waters experience intense shipping and offshore oil industry activities, which often result in marine pollution from oil spills. These spills damage marine ecosystems, disrupt sea transportation, cause organism mortality, and reduce both fishery production and marine tourism. Due to the significant environmental risks posed by oil in marine environments, effective and sustainable recovery technologies are essential. This study presents the development and performance analysis of a floating oil skimmer system integrated with renewable energy. A barge-type floating platform was selected as the optimal design due to its high buoyancy, low resistance, and good stability and seakeeping characteristics for small-scale applications compared with a catamaran. Experimental results show that the oil skimmer achieves optimum performance at a rotational speed of 120 RPM, collecting 1322 mL of oil within 5 minutes, which is equivalent to 264.4 mL/min or approximately 2.2 mL per revolution. If this performance is maintained consistently, the potential oil recovery capacity is 380.16 L/day. The results further demonstrate that increasing rotational speed improves recovery up to an optimum point, beyond which performance declines at higher speeds due to reduced contact time and increased turbulence. Regarding the energy source, only solar panels are considered feasible, whereas wind turbines are excluded due to their large dimensions, which compromise stability requirements. Additionally, this research contributes to the development of an autonomous oil skimmer capable of self-sufficient energy production, providing an efficient and environmentally friendly solution for oil spill recovery in Indonesian waters.

1. Introduction

Indonesian waters are among the regions with highly intensive shipping activities and offshore oil industries. This condition makes Indonesian waters vulnerable to marine pollution, particularly from oil spills. Historical records show at least 36 large-scale oil spill incidents that occurred between 1975 and 2004, ten of which took place at PT Pertamina's operational sites [1], [2]. In the past seven years (2018–2024) alone, there have been at least seven major oil spill incidents, including: a subsea pipeline leak of PT Pertamina in Balikpapan Bay in 2018, which caused severe damage to the marine ecosystem and resulted in five fatalities [3], [4]; a work accident at the Offshore North West Java (ONWJ) oil field owned by PT Pertamina in 2019 that led to pollution reaching the Karawang waters, West Java [5], [6]; an oil spill from the vessel MT Golden Pearl XIV in the Parepare waters in 2019 [7]; a drilling well leak of Pertamina Hulu Energi in the Kepulauan Seribu area in 2020 [8]; an oil spill at the Pertamina Cilacap refinery in 2021 [9]; an oil and gas leak in the Natuna area in 2023 [10]; and routine oil spill incidents occurring in the Riau Archipelago, including Batam and Bintan, which have persisted for several decades [8], [11]. In addition to these major incidents, there are still many small-scale oil spills that are not officially recorded or publicly reported.

Oil spills in the ocean have serious impacts on the environment and socio-economic activities. These impacts include damage to marine ecosystems, disruption of transportation routes, death of marine organisms, fish migration, and a decline in fisheries production and marine tourism [12], [13]. To address these issues, various oil spill recovery methods have been developed. One of the most widely used methods is the oil skimmer, a technology designed to remove oil from the water surface based on the principle of absorption or collection through various mechanisms such as belt, drum, disk, wire, vacuum, or pipe systems [14-17]. The use of booms and skimmers for marine oil spill recovery is considered environmentally friendly, as it does not cause harm to the marine ecosystem [18]. The performance of drum-type oil skimmers increases by

approximately 25% when sponge materials are used [19]. Furthermore, higher skimmer rotational speeds lead to increased oil recovery, but the efficiency tends to decrease [20].

However, most developments in oil skimmer technology currently remain focused on applications in industrial environments, with research directions aimed at improving efficiency and recovery methods, such as device design, rotation speed, operating temperature, oil viscosity and layer thickness, skimmer material and structure, as well as spill detection and location tracking methods [15-17], [21-27]. Considering the high frequency of marine oil spills and their significant impacts, particularly given that the allowable oil content in discharged water is limited to 15 ppm according to MARPOL 73/78 Annex I [28], [29], it is therefore necessary to develop an innovative floating-type oil skimmer technology specifically designed for marine oil pollution mitigation.

This study aims to design and test a prototype of a floating oil skimmer with the advantage of utilizing renewable energy as a power source. This innovation is expected to improve operational efficiency as it does not require fossil fuels. The use of renewable energy is highly relevant for marine implementation, considering that the marine environment provides abundant energy sources such as wind and solar energy. The scope of this research discussed in this paper includes the design of a floating oil skimmer equipped with effectiveness testing in separating oil on calm water surfaces and stability testing of the floating platform through an inclining test. Through these stages, it is expected to obtain comprehensive design results of the floating oil skimmer that can serve as a basis for further development.

2. Method

This research employs simulation and experimental methods through several main stages, including design, fabrication, testing, simulation, and renewable energy system calculations, as shown in more detail in Figure 1. The research begins with data collection, followed by the design of a floating oil skimmer system, which is divided into three main aspects: floating platform design, oil skimmer design, and renewable energy system design. The floating platform design includes resistance analysis followed by stability analysis, which is evaluated against the required criteria to ensure compliance with IMO 2008. If the criteria are not met, the design is revised iteratively until acceptable. Once satisfied, the process continues with seakeeping analysis and a further check against operability criteria or other requirements related to the small floating platform. In parallel, the oil skimmer design proceeds through model fabrication and test preparation stages, while the renewable energy system involves energy storage calculations and the determination of wind turbine and solar panel requirements.

The next stage involves testing and observing the oil skimmer performance, followed by a comparison of the initial results with relevant previous studies on the performance of drum-type oil skimmers [19], [30]. If the results are not valid, the process loops back to the preparation stages for refinement. If valid, the data are processed to evaluate key parameters such as weight, power consumption, and performance. Additionally, a feasibility analysis of the renewable energy system is conducted. Finally, the results are discussed comprehensively to draw conclusions, marking the end of the research process.

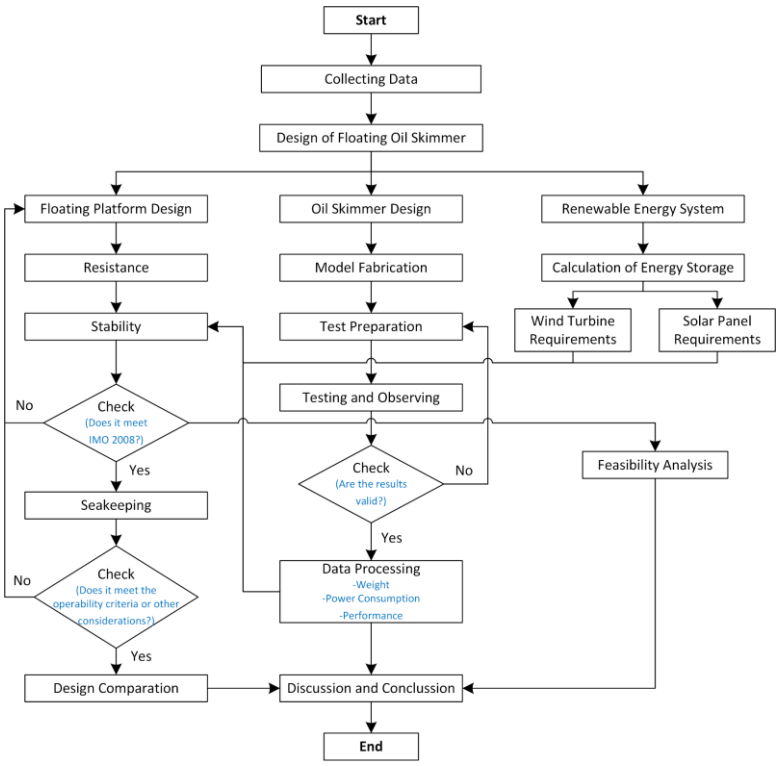

Figure 1. Flow chart of the research

The initial design of the floating oil skimmer is presented in Figure 2. Seawater contaminated with oil (effluent) is pumped into the floating platform and directed to the skimmer tank. The tank is designed based on the corrugated plate interceptor (CPI) principle, which utilizes differences in fluid density [31], allowing oil to rise to the surface while water remains at the bottom. The treated water is then transferred to the separator chamber and subsequently discharged back

into the sea, with the maximum allowable oil content limited to 15 ppm. Meanwhile, the oil accumulated on the surface is collected using a drum-type skimmer made of hydrophobic–oleophilic polymer materials [32], [33] driven by an electric motor, and stored in the oil storage tank beneath the main deck of the floating platform.

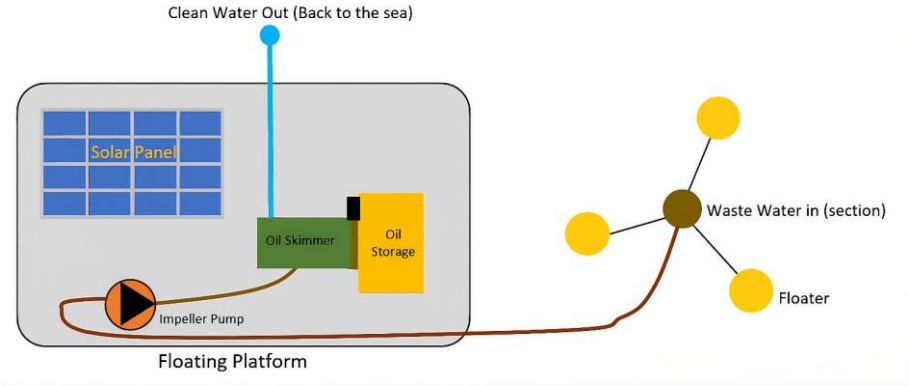

Figure 2. Sketch of the floating oil skimmer

To determine the optimal floating platform design, hydrodynamic analyses were conducted, including resistance, stability, and seakeeping. The resistance was calculated using the Holtrop method based on the following general equation [34-36]:

$$R_T = R_F(1+k1) + R_{APP} + R_W + R_B + R_{TR} + R_A \quad (1)$$

where:

R_F = Frictional resistance based on the ITTC–1957 formulation (kN)
$1+k1$ = Form factor representing viscous resistance related to the hull
R_{APP} = Appendage resistance (kN)
R_W = Wave resistance (kN)
R_B = Additional pressure resistance due to the bulbous bow near the water surface (kN)
R_{TR} = Additional pressure resistance due to the immersed transom (kN)
R_A = Correlation allowance for model-ship (kN)

For stability analysis, load cases are first defined, followed by the application of the governing equation [37]:

$$GZ = GM \sin \delta\phi \quad (2)$$

where:

GM = Metacentric height, the distance between points G and M (m)
$\delta\phi$ = Heel angle (°)

Seakeeping analysis is conducted using the following equation [38], [39]:

$$X_p = \frac{a_0}{\omega e^2} \quad (3)$$

where:

X_p = Motion amplitude; *heave* (m), *pitch* (rad), *roll* (rad)
a_0 = Acceleration amplitude; *heave* (m/s²), *pitch* (rad/s²), *roll* (rad/s²)
ωe = Encounter frequency (rad/s)

The power supply for the pump and skimmer motor is designed to utilize renewable energy, particularly solar energy. The integration of a wind turbine may be considered as an additional option, as combining two different renewable energy sources can enhance energy reliability. However, this option is only feasible if the designed floating platform meets the required criteria for wind turbine installation. The generated electrical energy is stored in batteries installed on the main deck.

3. Results and Discussion

The design of the floating oil skimmer in this study consists of three main components: the oil skimmer, the floating platform, and the renewable energy source, as shown in Figure 3.

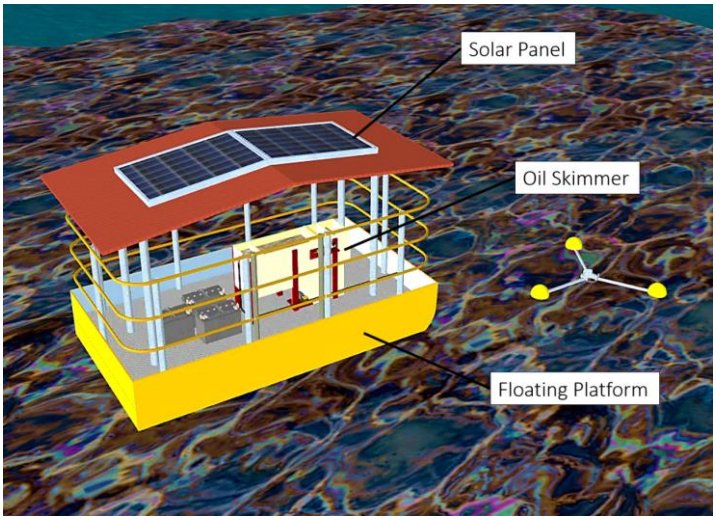

Figure 3. Floating oil skimmer design

3.1. Oil Skimmer

The oil skimmer is designed with dimensions of 0.9 m in length, 0.27 m in width, and 0.49 m in height, with the weight of 72.5 kg as shown in Figure 4(a). The oil skimmer is designed to include an oil-water separator of the corrugated plate interceptor (CPI) type. The working scheme of the oil skimmer is shown in Figure 4(b), where oily water is pumped from the sea surface into the oil skimmer tank. The oil skimmer tank functions as an oil-water separator of the CPI type, which is selected because it can quickly separate oil and water when oily water passes through the CPI plate arrangement. Based on the pressure difference principle, the oily water entering the CPI plates causes the oil, which has a lower density, to move upward to the surface, while the water, which has a higher density, is directed downward. The oil pushed to the surface is collected using a drum-type oil skimmer, while the water directed downward flows to the output channel and is returned to the sea. The drum oil skimmer uses an oleophilic-hydrophobic material due to its high oil affinity and water-repellent properties, similar to a lotus leaf.

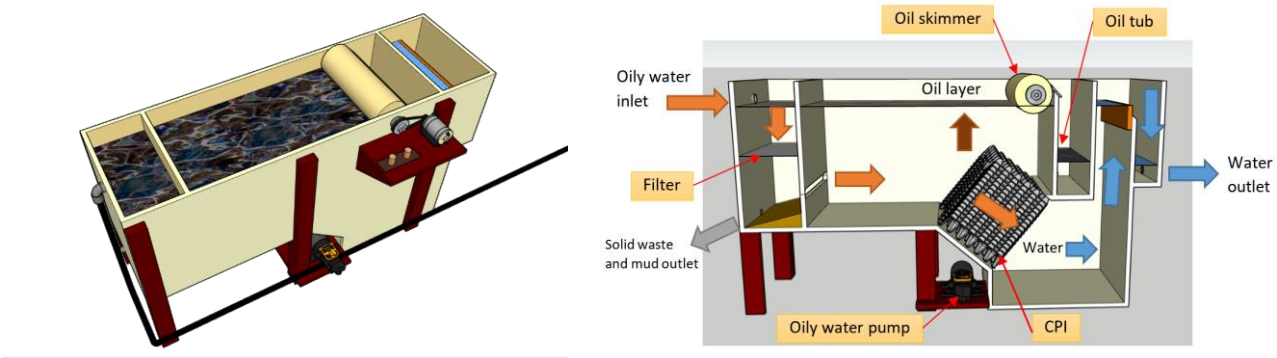

(a) (b)

Figure 4. (a) Oil skimmer design, (b) Working scheme

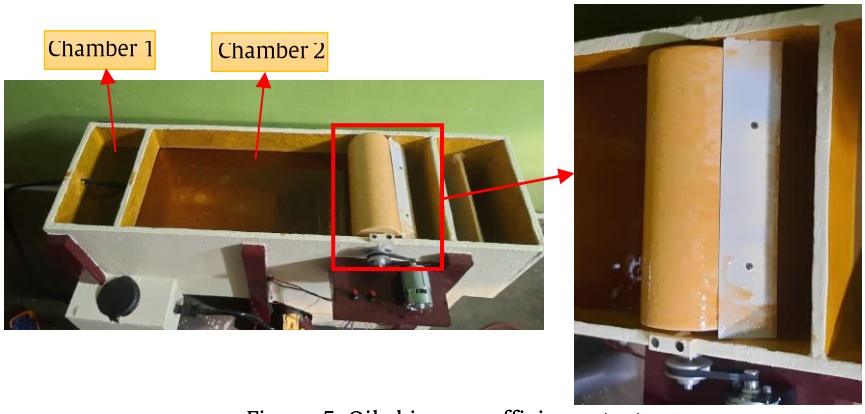

Figure 5. Oil skimmer efficiency test

After the design process, a full-scale (1:1) model test was conducted to determine the efficiency of the oil skimmer. The initial testing phase is presented in this paper. A pump with a capacity of 5 liters per minute was used to transfer oily water from the storage container into the oil–water separator tank. In Figure 5, the oil-water separator tank consisted of two sections: Chamber 1 served as the initial separator for oily water mixed with solid impurities and mud drawn in by the pump, while Chamber 2 functioned as the main separator of oil and water using corrugated plate interceptor (CPI) plates. The test results showed that oil and water separation began to occur in Chamber 1 due to the difference in density between oil and water, but it was not yet effective. Effective separation occurred in Chamber 2, where the CPI plates successfully separated oil molecules from water, causing the oil to rise to the surface while clean water flowed into the next compartment and then to the outlet. The oil layer on the surface of Chamber 2 was then skimmed using a drum-type oil skimmer. The results of the oil skimmer efficiency test are presented in Table 1.

Table 1. Results of the oil skimmer efficiency test

No	Rotation Speed (RPM)	Time (minutes)	Amount of Oil (mL)
1	60	5	1275
2	120	5	1322
3	180	5	543
4	240	5	201
5	300	5	-

The test results in Table 1 show that the amount of oil collected by the oil skimmer over 5 minutes reached its highest value at a speed of 120 RPM, amounting to 1322 mL. It then sharply decreased at higher speeds, with 543 mL at 180 RPM and 201 mL at 240 RPM, while no oil was collected at 300 RPM. These results clearly indicate that the optimum efficiency of the oil skimmer occurs at 120 RPM. At this condition, the oil skimmer can collect 264.4 mL/min, which is equivalent to approximately 2.2 mL per revolution.

The test results also show that the efficiency of the oil skimmer increases with rotational speed up to an optimum point and then decreases significantly thereafter due to reduced contact time between the skimmer surface and the oil layer, as well as increased turbulence around the collection surface. These findings are consistent with previous studies on innovations in oil skimmer machines for removing liquid contaminants [20]. During the experiments, it was observed that at higher rotational speeds, the boundary layer around the skimmer surface becomes more turbulent, causing the oil to be displaced away from the skimmer surface, while water adheres more easily due to higher shear forces.

3.2. Renewable Energy-Powered System

Calculation of Energy Storage (Battery) Requirements

The calculation of energy requirements was conducted to determine the capacity and number of batteries needed. During the oil skimmer testing, measurements of current and voltage were taken for the DC 775 oil skimmer motor and the 100 PSI oily water pump. The results showed that the maximum voltage measured on the motor was 10.72 V at a rotation speed of 300 RPM, while the maximum voltage on the pump was 11.34 V. The current recorded using a digital multimeter indicated that both components operated at 1 A. It was also observed that the motor and pump were connected to a DC voltage regulator with an input range of 5–35 V and a current capacity of 5 A, which was used to control the rotational speed.

The test results were used as the basis for calculating the electrical energy requirements, in which the voltage values for the motor and pump were standardized to 12 volts and the current to 1 A. Table 2 shows the calculation of the energy requirements for the oil skimmer system.

Table 2. Energy requirement calculation

No	Component	Voltage (V)	Current (A)	Power (W)	Operating Time (h)	Energy (Wh)
1	Oil skimmer motor	12	1	12	24	288
2	Oily water pump	12	1	12	24	288
3	Cooling system pump	12	1	12	24	288
					Total	**864**

Based on Table 2, the total maximum energy requirement is 864 Wh. However, a safety factor of 20% should be added to anticipate possible power surges, such as those occurring in the cooling system. For energy storage, batteries with a specification of 12 volts and a capacity of 32 Ah are used. The calculation of the required number of batteries is presented as follows:

Qty = Total power / battery storage capacity
= 864 + 20% x 576 / (12*32)
= 1036.8 / 384
= 2.7 units, rounded up to 3 units.

Solar Panel Requirements

The capacity of the solar panel used is 100 watt peak (Wp), with an optimal electricity generation efficiency of 80%, resulting in 80W being used as the basis for calculating the battery charging time from an empty state, as follows:

T = battery storage capacity / optimal solar panel capacity
= 384 Wh / 80 W

= 4.8 h

If the effective sunlight duration is approximately 7 hours per day, one solar panel can charge more than one battery from an empty state, although in practice the batteries are not charged from a fully depleted condition but from about 30% of their capacity. Therefore, two solar panels are considered sufficient to charge three batteries. Additionally, a safety component in the form of a load resistor is included to dissipate excess electrical power generated. This measure aims to protect the batteries from damage caused by overcharging.

Wind Turbine Requirements

The wind turbine is designed as a Vertical Axis Wind Turbine (VAWT), commonly represented by types such as Darrieus, Savonius, and Helical. The planned power output of the wind turbine is 100 Wp, with an estimated power coefficient (Cp) of 0.38, based on reference [40] hich utilizes a three-bladed NACA 0021 airfoil operating at a Tip Speed Ratio (TSR) of 2.5. Using the power calculation, the swept area can be determined by applying Equation (4).

$$A = \frac{P}{\frac{1}{2}\rho C_p v^3} \tag{4}$$

where:

A = swept area (m^2)
P = turbine power (watt)
ρ = air density (1.225 kg/m^3)
Cp = power coefficient
v = wind speed (m/s)

The wind speed over Indonesian sea surfaces reaches its seasonal peak in August at 5.42 m/s, with an annual average of 3.76 m/s [41] To generate 100 Wp, the required swept area of the VAWT is A = 8.08 m^2 for the average wind speed (v = 3.76 m/s) and A = 2.70 m^2 for the maximum wind speed (v = 5.42 m/s). Based on these swept areas, the VAWT dimensions in terms of height (H) and diameter (D) can be determined using several H/D ratios. The swept area can be expressed as A = H·D. By introducing the ratio H/D, the equation can be rewritten as:

$$A = r \cdot D^2 \tag{5}$$

where:

r = ratio (H/D)

By applying Equations (4) and (5), various feasible VAWT dimensions are obtained, as presented in Table 3.

Table 3. VAWT dimension variations based on wind speed

v (m/s)	Ratio	H (m)	D (m)
3.76 (average)	0.5	2.1	4.02
	1	2.84	2.84
	2	4.02	2.01
	3	4.92	1.64
	4	5.69	1.42
5.42 (maximum)	0.5	0.82	1.64
	1	1.16	1.16
	2	1.64	0.82
	3	2.01	0.67
	4	2.32	0.58

Based on Table 3, it is evident that the VAWT requires a relatively large dimension to generate the necessary power, whereas the floating platform is designed with a length of only 2.5 m and a width of approximately 1.4 m. Therefore, the VAWT for application on the floating oil skimmer is considered unfeasible. Even when simulated using the most optimal dimension ratio, r = 3, at maximum wind speed, where the VAWT dimensions are D = 0.95 m and H = 2.85 m, the stability performance of the floating platform does not meet IMO criteria due to the excessive height of the wind turbine. For comparison, the installation of solar panels alone requires a height of approximately 1.2 m above the main deck, as a higher placement would reduce the floating platform′ s stability and fail to meet IMO 2008 criteria [42].

3.3. Floating Platform

The floating platform serves as the floating base for the oil skimmer components. Therefore, a reliable floating platform is required in terms of hydrodynamics, such as resistance, stability, and seakeeping. A comparative study was conducted on several floating platform models, including catamaran and barge types. Table 4 presents a comparison of the dimensions of five floating platform designs.

The comparison of dimensions in Table 4 shows that the barge type outperforms the catamaran type because it has a larger displacement, which indicates greater buoyancy, and a smaller wetted surface area compared to the catamaran even

when the dimensions are similar or slightly smaller. The designs of the five floating platform types are presented in Table 5 and Figure 6 show the corresponding resistance results.

Table 4. Comparison of floating platform dimensions

Parameter	Unit	Catamaran 1	Catamaran 2	Barge 3	Barge 4	Catamaran 5
Length Over All (LOA)	m	2.5	3	2.5	2.5	2.5
Length of Water Line (LWL)	m	2.5	3	2.4	2.5	2.5
Breadth (B)	m	1.4	1.4	1.4	1.4	1.4
Height (H)	m	0.6	0.8	0.4	0.4	0.6
Draft (T)	m	0.4	0.424	0.25	0.25	0.4
Diplacement (∆)	kg	630.9	645.4	757.5	816.4	655.2
Deck Area	m^2	3.5	4.2	3.5	3.5	3.5
Wetted Surface Area (Ws)	m^2	5.29	5.79	4.682	4.952	5.387

Table 5. Comparison of design shapes

Name	Perpective-Bottom View	Perpective-Side View
Catamaran 1	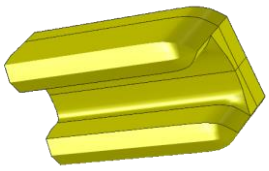	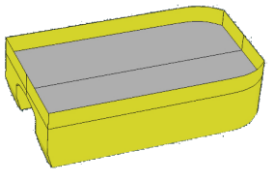
Catamaran 2	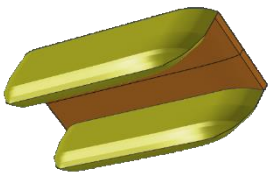	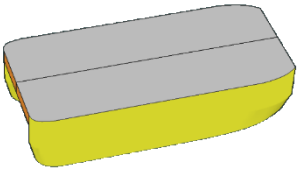
Barge 3		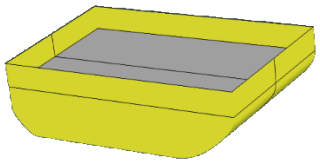
Barge 4		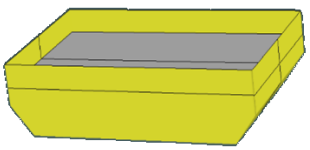
Catamaran 5	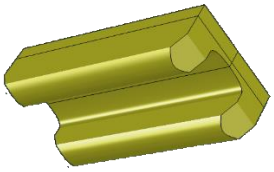	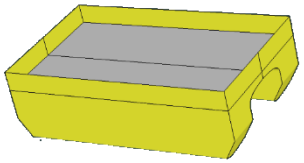

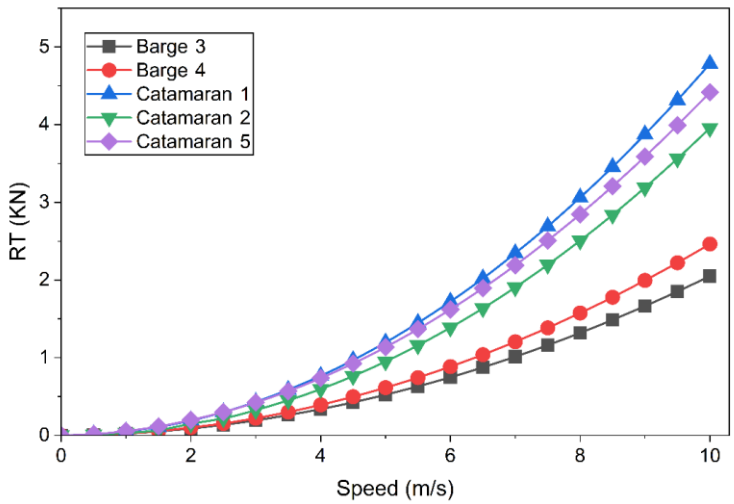

Figure 6. Comparison of total resistance

Based on the predicted resistance results, it is evident that the barge hull performs better than the catamaran, with the Barge 3 model exhibiting the lowest resistance. This finding reinforces the previous observation that, in terms of dimensions, the barge model outperforms the catamaran. A larger displacement allows for a greater portion of deadweight, considering that the lightship weight of each floating platform model does not differ significantly due to their similar dimensions.

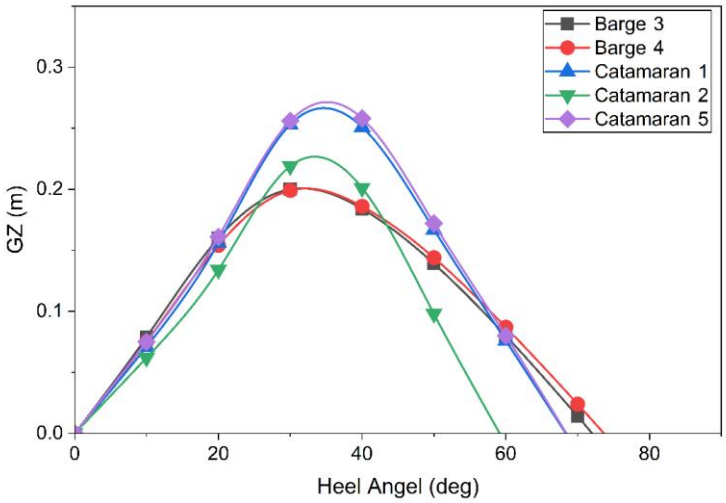

Figure 7. Comparison of righting moment (GZ)

The stability comparison is presented in the righting moment (GZ) graph in Figure 7 and the stability criteria in Table 6. Figure 7 shows that all models reach a maximum GZ at angles above 30°, with the highest GZ produced by the Catamaran 5 model. In terms of stability, the catamaran models exhibit better righting moments compared to the barge models. According to the IMO stability criteria [42] presented in Table 6, one floating platform model, Catamaran 2, does not meet the stability requirement for the area under the GZ curve from 0° to 30°, producing only 3.08 m·deg while the minimum standard is 3.151 m·deg. Apart from this, the other four floating platform models meet the criteria, even though the standard is more applicable to vessels with a length of ≥ 24 m. Moreover, the GM0 values of these four platforms exceed the minimum standard significantly, indicating that their stability performance is very good.

Table 6. Stability criteria evaluation

Stability Criteria (IMO, 2008)		Catamaran 1		Catamaran 2		Barge 3		Barge 4		Catamaran 5	
Parameter	Req.	Actual	Status	Actual	Status	Actual	Status	Actual	Status	Actual	Status
Area 0^0 to 30^0 (m.deg)	≥ 3.151	3.55	Acc.	3.08	Fail	3.44	Acc.	3.32	Acc.	3.65	Acc.
Area 0^0 to 40^0 (m.deg)	≥ 5.157	6.16	Acc.	5.28	Acc.	5.40	Acc.	5.28	Acc.	6.32	Acc.
Area 30^0 to 40^0 (m.deg)	≥ 1.719	2.61	Acc.	2.20	Acc.	1.96	Acc.	1.96	Acc.	2.67	Acc.
GZ_{max} at 30^0 or greater (m)	≥ 0.2	0.27	Acc.	0.23	Acc.	0.20	Acc.	0.20	Acc.	0.27	Acc.
Angle of GZ_{max} (deg)	≥ 25	34.50	Acc.	33.60	Acc.	31.80	Acc.	31.80	Acc.	35.50	Acc.
GM_0 (m)	≥ 0.15	0.40	Acc.	0.35	Acc.	0.45	Acc.	0.43	Acc.	0.42	Acc.

The next comparative study focuses on seakeeping, which is the analysis of floating platform motions under static conditions and free from mooring effects. This analysis aims to examine the platform's motion behavior under external forces when the floating oil skimmer is in operation. Due to the small size of the floating platform, seakeeping evaluation based on the acceptance criteria proposed by [43-45]. could not be applied. Therefore, the comparative study was conducted by analyzing the motion behavior in response to waves. The results of the station-keeping analysis for heave, roll, and pitch motions are presented in Figures 8 to 10.

The heave motion shown in Figure 8 is the result of a simulation with slight wave conditions (Hs = 1 m) in the head sea direction. The heave magnitude of the barge models is better compared to the catamaran models, while the motion periods are relatively similar. The roll motion presented in Figure 9 corresponds to a simulation under smooth wave conditions (Hs = 0.5 m) in the beam sea direction. In this figure, the roll motion of the catamaran models is superior to that of the barge models. The twin-hull design of the catamaran provides greater damping during roll motion, resulting in a smaller roll magnitude compared to the barge. Figure 9 shows that the lowest roll motion is produced by Catamaran 1 and Catamaran 5, both exhibiting the same motion amplitude. Figure 10 presents the pitch motion comparison of the floating platforms under slight wave conditions (Hs = 1 m) in head sea direction, where the best pitch performance is observed in the barge models.

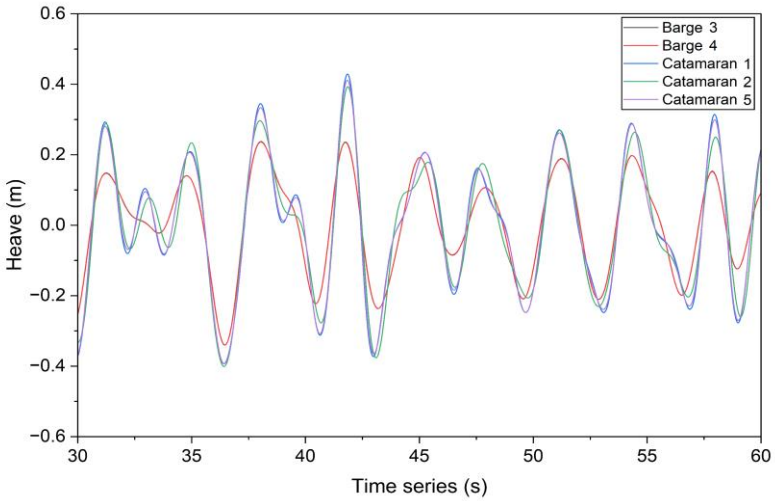

Figure 8. Comparison of heave motion

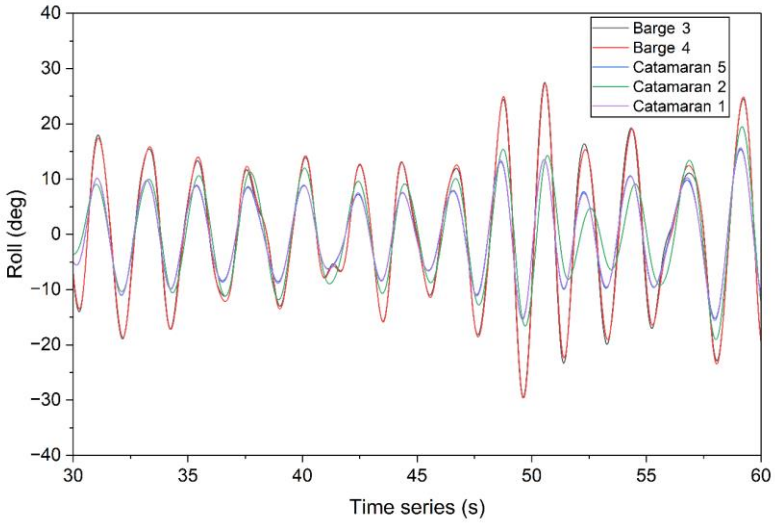

Figure 9. Comparison of roll motion

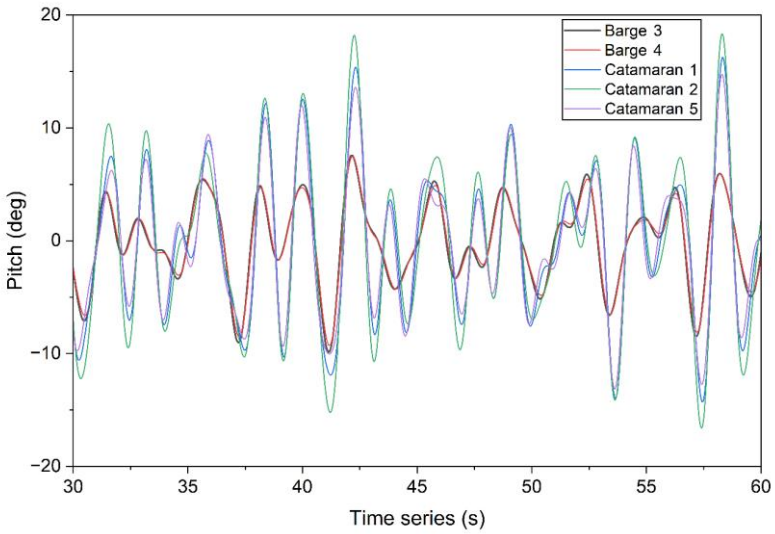

Figure 10. Comparison of pitch motion

In the seakeeping analysis, comparing the motion magnitudes shown in Figures 8 to 10 is not sufficient. Therefore, a comparison of the Root Mean Square (RMS) values, which represent the statistical mean of all motion cycles of the floating platform, is presented in Table 7. From the table, the smallest RMS value for heave motion is produced by Barge 4, which is nearly identical to that of Barge 3. Across different headings, the largest heave motion occurs at the beam sea for all floating platform models, due to the platform being in a static condition. The smallest RMS value for roll motion is produced by Catamaran 5, while the smallest RMS for pitch motion is produced by Barge 4. Pitch motion is more pronounced when the platform encounters waves in the following sea direction.

Based on the comparative study of dimensions, shape, resistance, stability, and seakeeping under static conditions, it can be concluded that the barge models perform better than the catamaran. Among the barge models, Barge 3 is identified as the most suitable design for the floating oil skimmer platform.

Table 7. Comparison of seakeeping rms values

Name	Heading (deg)	RMS Motion: Smooth (Hs 0.5 m)			RMS Motion: Slight (Hs 1 m)			RMS Motion: Modarate (Hs 2 m)		
		Heave (m)	Roll (deg)	Pitch (deg)	Heave (m)	Roll (deg)	Pitch (deg)	Heave (m)	Roll (deg)	Pitch (deg)
Barge 3	0	0.119	0	7.05	0.246	0	8.31	0.498	0	11.25
	90	0.122	12.34	3.15	0.246	13.81	3.52	0.494	18.08	4.61
	180	0.118	0	3.38	0.246	0	4.3	0.497	0	6.1
Barge 4	0	0.118	0	6.75	0.246	0	7.99	0.497	0	10.85
	90	0.121	12.3	3.09	0.246	13.79	3.45	0.494	18.07	4.51
	180	0.118	0	3.25	0.246	0	4.17	0.497	0	5.93
Catamaran 1	0	0.163	0	8.03	0.288	0	9.12	0.546	0	12.1
	90	0.17	7.17	3.68	0.289	8.29	3.98	0.542	11.06	5.13
	180	0.163	0	5.93	0.288	0	6.87	0.545	0	9.25
Catamaran 2	0	0.167	0	6.88	0.291	0	7.96	0.548	0	10.66
	90	0.179	7.78	2.52	0.295	9	2.78	0.547	11.98	3.61
	180	0.156	0	6.67	0.283	0	7.66	0.541	0	10.23
Catamaran 5	0	0.159	0	7.45	0.285	0	8.51	0.543	0	11.34
	90	0.17	7.12	3.34	0.289	8.22	3.61	0.542	10.98	4.66
	180	0.159	0	5.43	0.285	0	6.34	0.543	0	8.59

4. Conclusion

The floating oil skimmer was designed using the Barge 3 model as the floating platform because it has advantages including high buoyancy, lower resistance, and good stability and seakeeping performance. The oil skimmer system is equipped with a corrugated plate interceptor (CPI) type oil-water separator to accelerate the separation of oil and water, allowing oil that accumulates on the surface to be easily collected by a drum-type oil skimmer. Electrical energy is supplied by two 100 Wp solar panels charging three 12 V 32 Ah hybrid batteries. The energy storage capacity is sufficient for the operation of the entire system, including the oily water pump, the DC 775 motor driving the skimmer drum, and the cooling system pump. Efficiency testing of the oil skimmer showed that the highest oil collection volume was achieved at 120 RPM, with an average oil collection of 2.2 mL per revolution. However, the oil skimmer effectiveness did not meet the planned target, which is to collect at least 4.2 mL per revolution to balance the oil entering Chamber 2 with the oil collected. Excessive accumulation of oil on the surface of Chamber 2 affects the CPI plate' s efficiency in separating oil and water, reducing the clarity of the water discharged from the oil skimmer. Therefore, improvements are needed, including the use of skimmer material with better oleophilic properties, adjustment of the skimmer position to reduce oil being displaced due to increased boundary layer turbulence of skimmer drum while in high rotation, optimization of the scraper design with more efficient materials and shape to collect oil more effectively and reduce resistance, and the addition of one oil skimmer unit in Chamber 1.

Acknowledgements

The authors wish to express gratitude to the Directorate of Research and Community Service (DPPM) of the Ministry of Higher Education, Science, and Technology for funding this research, as well as to the Rector and the academic community of the Bacharuddin Jusuf Habibie Institute of Technology for providing facilities and support throughout the research process.

References

[1] E. B. Haryani, "Oil Pollution At Sea and Compensation Claims," *Sekolah Pasca Sarjana IPB*, no. Pps 702. Institut Pertanian Bogor, Bogor, pp. 1–16, 2005.
[2] S. Maemunah, A. S. Widjaya, Hairuddin, A. Kirom, J. Punuh, and A. Widianto, *Indonesia Bangkrut*. Jakarta Selatan: Jaringan Advokasi Tambang (JATAM), 2005.
[3] S. Amelia, "Oil Spill in Balikpapan Bay Causes Environmental Problems," *Seri Publ. Pembelajaran Pendidik. Lingkung. Hidup*, vol. 1, no. 1, pp. 2–4, 2022.
[4] Seliyana, B. Anzward, and Rosdiana, "Legal Responsibility of PT. Pertamina Due To Pipe Leakage In Teluk Balikpapan," *J. Lex Suprema*, vol. 1, no. 2, pp. 1–17, 2019.
[5] M. A. B. Amffa, M. F. Arsy, and F. M. Assidiq, "Analysis of the Impact of Oil Spills on Coastal Communities in Karawang from Legal and Environmental Perspectives," *Riset Sains Dan Teknologi Kelautan*, vol. 6, no. 1, pp. 86–89, 2023, doi: https://doi.org/10.62012/sensistek.v6i1.24261.
[6] S. Margareta and W. Boediningsih, "Corporate Liability for Environmental Pollution Reviewed Based on the Environmental Protection and Management Law," *Jurnal Hukum Indonesia*, vol. 2, no. 1, pp. 1–13, 2023, doi: https://doi.org/10.58344/jhi.v2i1.10.
[7] A. A. T. Jadda, S. Mansur, H. Hamzah, and Kaswin, "The Role of the Environmental Agency in Controlling Pollution Due

to Oil Spills by Pertamina in Parepare City (in Indonesian)," *Madani Legal Review.*, vol. 6, no. 1, pp. 1–20, 2022. doi: https://doi.org/10.31850/malrev.v6i1.1705
[8] T. Redaksi, "4 Cases of Oil Spills in Indonesian Waters," *lautsehat.id*, 2021. [Online]. Available: https://lautsehat.id/peristiwa/lautsehat/4-kasus-tumpahan-minyak-di-perairan-indonesia/
[9] M. Wibowo, "Computational Modeling of Oil Spill Pollution Distribution in Cilacap Seawaters," *Jurnal Teknologi Lingkungan*, vol. 19, no. 2, p. 191, 2018.
[10] R. N. R. Nadeak, "Analysis ofOil Spill Distribution andMovement Based on 2D Hydrodynamic Modeling in Natuna Sea Waters, Riau Islands Province," Universitas Diponegoro, Semarang, 2023.
[11] I. Damai Agusthin, S. Putri Ramadhani, and M. Adymas Hikal Fikri, "Mitigation of Oil Spills in the Riau Islands Sea Waters Based on the Law of the Sea Convention (in Indonesian)," *Jembatan Hukum : Kajian Ilmu Hukum, Sosial Dan Administrasi Negara*, vol. 1, no. 2, pp. 186–208, 2024, doi: https://doi.org/10.62383/jembatan.v1i2.264
[12] N. A. Annisa, P. Vionica, and U. Kamal, "Environmental Impact Analysis of Coastal Areas Due to Oil Spill in Karawang," *Media Huk. Indones.*, vol. 2, no. 2, pp. 192–196, 2024, doi: https://doi.org/10.5281/zenodo.11261952.
[13] H. Grace, A. Belle, G. Margareth, T. Adefinola, and N. Febrayen, "Tanker Ship Accidents: Risks of Oil/Chemical (Hazardous Materials) Spills Affecting the Marine Environment, Response Challenges, and Tanker Safety Design Regulations," vol. 2, no. 1, pp. 326–346, 2025.
[14] V. Sathiyamoorthy, K. Arumugam, M. Arun Pragathish, B. N. Barath, M. Baskar, and S. Balamurugan, "A review of mobile oil skimmer," *International Journal of Engineering and Technology*, vol. 7, no. 3.34 Special Issue 34, pp. 58–60, 2018, doi: https://doi.org/10.14419/ijet.v7i3.34.18716.
[15] S. S. Godawarikar and A. T. Gavhane, "Literature Review On Oil Recovering Skimmer From The Surface of Water," *Int. Res. J. Eng. Technol.*, vol. 07, no. 03, pp. 3956–3960, 2020.
[16] M. Đordevic, Đ. šabalja, Đ. Mohovi´c, and D. Brci´, "Optimisation Methodology for Skimmer Device Selection for Removal of the Marine Oil Pollution," *Journal of Marine Science and Engineering,* vol. 10, no. 7, pp. 925–941, 2022. doi: https://doi.org/10.3390/jmse10070925
[17] S. Supriyono1 and D. T. Nurrohman, "Floating oil skimmer design using rotary disc method," in *Journal of Physics: Conference Series*, Chicago: IOP Publishing, 2019, pp. 1–8. doi: https://doi.org/10.1088/1742-6596/1450/1/012046.
[18] D. N. L. Huynh *et al.*, "Booms and skimmers for oil spill recovery: Perspective analysis from lab scale to practical applications," *Marine Pollution Bulletin*, vol. 224, p. 119128, 2026, doi: https://doi.org/10.1016/j.marpolbul.2025.119128.
[19] M. F. Khalil, I. El-boghdady, and E. R. Lotfy, "Oil-recovery performance of a sponge-covered drum skimmer," *Alexandria Engineering Journal*, vol. 61, no. 12, pp. 12653–12660, 2022, doi: https://doi.org/10.1016/j.aej.2022.06.011.
[20] S. Patil, P. Desai, S. Lavate, S. Patil, and S. Patil, "Innovative oil skimmer machine for liquid contaminant removal: An environmental friendly approach," *Regional Studies in Marine Science*, vol. 86, p. 104184, 2025, doi: https://doi.org/10.1016/j.rsma.2025.104184.
[21] R. K. Nanwatkar, G. J. Sapakale, B. P. Korke, S. T. Waghmare, and N. R. Ansari, "Design and Experimental Analysis of Oil Skimmer for Water Filtration," *Journal of Science and Technology*, vol. 06, no. 01, pp. 604–613, 2021. https://jst.org.in/index.php/pub/article/view/808
[22] D. Motorin, H. Roozbahani, and H. Handroos, "Development of a novel method for estimating and planning automatic skimmer operation in response to offshore oil spills," *Journal of Environmental Management*, vol. 318, p. 115451, 2022, doi: https://doi.org/10.1016/j.jenvman.2022.115451.
[23] Y. Kim, H. Kim, and D. Cho, "Evolutionary Approach to Optimal Oil Skimmer Assignment for Oil Spill Response : A Case Study," *Biomimetics*, vol. 9, no. 330, pp. 1–17, 2024. doi: https://doi.org/10.3390/biomimetics9060330
[24] R. Manivel and R. Sivakumar, "Materials Today : Proceedings Boat type oil recovery skimmer," in *Materials Today: Proceedings*, Elsevier Ltd., 2020, pp. 470–473. doi: https://doi.org/10.1016/j.matpr.2019.06.632.
[25] W. E. Odiete and J. C. Agunwamba, "Heliyon Novel design methods for conventional oil-water separators," *Heliyon*, vol. 5, no. 5, 2019, doi: https://doi.org/10.1016/j.heliyon.2019.e01620.
[26] B. Herren, M. C. Saha, M. C. Altan, and Y. Liu, "Funnel-Shaped Floating Vessel Oil Skimmer with Joule Heating Sorption Functionality," *Polymers (Basel).*, vol. 14, no. 11, 2022. doi: https://doi.org/10.3390/polym14112269
[27] Z. Mushtaq, I. Ali, R. Shah, S. S. Sani, and S. F. Su, "Detection , Localization and Analysis of Oil Spills in Water Through Wireless Thermal Imaging and Spectrometer Based," in *Wireless Personal Communications*, Springer US, 2020, pp. 679–698. doi: https://doi.org/10.1007/s11277-019-06880-3.
[28] IMO, "Annex I Regulations for the Prevention of Pollution by Oil (entered into force 2 October 1983)," *International Convention for the Prevention of Pollution from Ships (MARPOL)*, 1983.
[29] Ministry of Transportation of the Republic of Indonesia, *Prevention of Maritime Environmental Pollution*. Indonesia
[30] A. H. Hammoud and M. F. Khalil, "Performance of a rotating drum skimmer in oil spill recovery," in *Proceedings of the Institution of Mechanical Engineers, Part E: Journal of Process Mechanical Engineering*, Sage, London, 2003, pp. 49–57. doi: https://doi.org/10.1243/09544080360562981.
[31] CEW, "Corrugated Plate Interceptor," *Chemical Engineering World*, 2024. https://chemicalengineeringworld.com/corrugated-plate-interceptor/ (accessed Apr. 08, 2025).
[32] P. Formentín, L. K. Acosta, and L. F. Marsal, "Hydrophobic-oleophilic surfaces based on chemical modification of nanoporous alumina," *Materials Chemistry and Physics*, vol. 302, no. April, p. 127686, 2023, doi: https://doi.org/10.1016/j.matchemphys.2023.127686.
[33] S. W. Ko, J. Y. Moon, S. M. Bae, C. S. Kim, and C. H. Park, "A Sponge-Type oil skimmer for highly efficient removal of floating Oils: Superabsorbent and oleophilic sponge with Nano-Scale interface roughness," *Applied Surface Science*, vol. 606, p. 154750, 2022, doi: https://doi.org/10.1016/j.apsusc.2022.154750.

[34] J. Holtrop, "A statistical re-analysis of resistance and propulsion data," *International Shipbuilding Progress*, vol. 31, pp. 272–276, 1984. ttps://api.semanticscholar.org/CorpusID:111508867
[35] A. Yasim, R. K. Koentjoro Wibowo, and K. Priohutomo, "KAJIAN SINKRONISASI MESIN UTAMA DAN PROPELLER PADA KAPAL PERIKANAN PASCA REPARASI (STUDI KASUS KM. NELAYAN 2017-572)," *Wave Jurnal Ilmu Teknologi Maritim*, vol. 15, no. 1, pp. 11–20, Aug. 2021.
[36] E. D. Fuady, P. S. Asmara, and I. Sutrisno, "Ship Maneuvering Simulation to Determine Elements of Tugboat Handling: A Case Study of Paciran Port," *Kapal: Jurnal Ilmu Pengetahuan dan Teknologi Kelautan*, vol. 22, no. 3, pp. 162–173, 2025, doi: https://doi.org/10.14710/kapal.v22i3.74393.
[37] L. L. Goldberg, *Principles of Naval Architecture, second revision*, vol. I. Jersey City-US: Society of Naval Architects and Marine Engineers, 1988.
[38] R. F. Kusnadi, P. G. Widityo, A. Yasim, and B. Ali, "Analysis of the Effect of Bilge Keel on the Rolling Motion of Ro-Ro Ferry Ship Using the Strip-Theory Method," *ROTOR*, vol. 16, no. 1, pp. 15–20, 2023.
[39] A. Yasim, M. Soetardjo, and Mahrani, "Seakeeping Performance Analysis of A 5 GT Fishing Vessel After Hatch Modification and Main Engine Replacement (Case Study : KM. Nelayan 2017-572," *Jurnal Airaha*, vol. 14, no. 02, pp. 205–218, 2025, doi: https://doi.org/10.15578/ja.v14i2.780.
[40] M. Reza, "Investigation and Optimization on Effective Parameters of a H-Rotor Darrieus Wind Turbine , Using CFD Method," vol. 42, no. 9, pp. 3030–3046, 2023. doi: https://doi.org/10.30492/ijcce.2023.562396.5610
[41] M. R. Muskananfola, Jumsar, and A. Wirasatriya, "Spatio-temporal distribution of chlorophyll-a concentration, sea surface temperature and wind speed using aqua-modis satellite imagery over the Savu Sea, Indonesia," *Remote Sensing Applications: Society and Environment*, vol. 22, p. 100483, 2021, doi: https://doi.org/10.1016/j.rsase.2021.100483.
[42] IMO, *International Code of Intact Stability 2008*, 2020th ed. International Maritime Organization (IMO), 2020.
[43] Nordforsk, "Seakeeping Criteria." 1897.
[44] Det Norske Veritas Germanischer Lloyd, "DNVGL-RP-C205: Environmental Conditions and Environmental Loads," *DNV GL Recomm. Pract.*, no. August, pp. 1–259, 2017.
[45] API RP 2SK, *Design and Analysis of Stationkeeping Systems for Floating Structures*, Third Edit., no. May. Washington D.C: American Petroleum Institute, 2005.